Orclever Proceedings of Research and Development
https://doi.org/10.56038/oprd.v5i1.507
OR CLEVER Science & Research Group

Conference Article

Non-Newtonian Fluid Based Non-Linear Impedance Control for Robotic Manipulators

Oğuzhan AKBIYIK[1*2], Semih SEZER[3]

[1] Yıldız Technical University, Orcid ID: https://orcid.org/ 0009-0004-3722-0100.,
e-mail: oğuzhan. akbiyik@std.yildiz.edu.tr
[2] MCFLY Robot Teknolojileri A.Ş, Sarıyer, 34485 İstanbul, Turkey
[3] Yıldız Technical University, Orcid ID: https://orcid.org/0000-0002-5987-8980., e-mail: sezer@yildiz.edu.tr
* Correspondence: e-mail; mobile phone

Received 12 October 2024
Received in revised form 11 December 2024
In final form 16 December 2024

4th International Conference on Design, Research and Development
(RDCONF 2024)
December 19 - 20, 2024

Reference: Akbıyık, O., & Sezer, S. (2024). Non-Newtonian fluid based non-linear impedance control for robotic manipulators. Orclever Proceedings of Research and Development, 5(1), 84-98.

Abstract

The increasing presence of robots in sectors involving physically or mentally unhealthy tasks, such as high-repetition jobs, chemical synthesis, and high-temperature environments, has led to advancements in robotics for tasks requiring complex environmental interaction, such as grinding, polishing, and assembly. However, the structural rigidity of most industrial robots, which contrasts with the flexibility of human muscles, limits their effectiveness in such tasks. Impedance control, a widely studied framework for managing robot-environment dynamics, has been expanded to address these challenges but struggles with vibrations and collision dynamics. To address these issues without sacrificing flexibility, this study proposes integrating a non-Newtonian fluid-based damping element into impedance control, leveraging fluid dynamics to improve vibration damping and collision safety, enhancing robotic performance in interactive applications.

Keywords: *Impedance Control, Non-Newtonian Fluid, Robotic Polishing*

https://doi.org/10.56038/oprd.v5i1.507

1. Introduction

In recent years, particularly following the global pandemic of 2020, the transfer of human-performed, skill-intensive tasks to robotic systems has gained noticeable momentum in both industry and academia. However, research and efforts to enable robots to replicate human tasks have been ongoing since the introduction of optimal control theory in the 1980s. While robots have been widely utilized in industry, human motor skills and reasoning capabilities have generally outperformed robots, especially in handling complex tasks requiring interaction with the environment. A significant breakthrough in this field occurred in 1984 when Hogan [1] introduced the impedance control theory, which garnered substantial attention. Impedance control models the interaction between a robot and its environment as a virtual mass-damper-spring system, allowing indirect manipulation of the interaction by altering the system's parameters.

Initially adopted for robotic contact-rich tasks, this method evolved significantly over time. In 2006, Pyung Hun Chang [2] advanced the concept by introducing a nonlinear impedance model, incorporating time delays into the system to enhance the dynamics of robot collisions. Building on this, Chow Yin Lai [3], in 2012, developed a generalized nonlinear impedance model. By analytically determining parameter stability limits, he successfully reduced excessive forces during robot collisions.

Interestingly, one of the inspirations for this study came from a study outside the robotics field. In 2018, Abuobaker Gherbi [4] investigated the use of nonlinear viscous damping elements in structural control and vibration attenuation. His findings demonstrated that nonlinear damping elements offer superior vibration suppression and impact characteristics compared to their linear counterparts, providing valuable insights for robotic applications. Another out-of-field research on non-linear damping was presented in [6] by Golzar et al. Here, the authors designed a re-centring viscous damper with non-Newtonian damping and explored the contact damping characteristics of such a device. The findings were pointing to the fact that the viscous device provides consistent rate-dependent dissipative behaviour. In [5], researchers used a nonlinear viscous damping fluid in their polishing head design which had substantial improvements on vibration damping for polishing applications. Their approach however, limited the adaptability of damping characteristics since a physical fluid with fixed viscoelasticity is present in the end effector.

While these efforts on non-linear impedance formulations are substantial developments in the field, most of them lacks the intuitiveness, ease of implementation, and adaptation. Furthermore, the primary focus in most of them is a single objective, such as vibration compensation or collision dynamics enhancements, which are essentially two conflicting

https://doi.org/10.56038/oprd.v5i1.507

tasks since to dampen the vibrations, one must increase the stiffness and damping of the robot which in turn yields worse contact and collision characteristics. This work proposes to introduce a non-Newtonian Fluid based nonlinear damping model into the standard impedance model for robotic applications with complex dynamic contacts. This approach is intuitive and easy to implement, allowing the system to be tuned for specific applications and needs without dwelling into highly nonlinear models and optimization procedures. The model parameters can be designed to resist high-frequency, low-scale vibrations while accommodating low-frequency, high-scale forces or vice-versa. This capability is particularly critical in tasks such as collaborative robotic polishing, where vibration damping from the polishing head is necessary to maintain precision, but excessive damping must be avoided to ensure safety in scenarios where a human might contact the robot. Ou, Yang, et al [12]. proposed an end effector employing pneumatic-electric linear force control for polishing applications, as depicted in Figure 1. However, similar to the methodology presented in [5], their approach is inherently linear and hardware-centric, posing significant limitations in terms of adaptability and multitasking capabilities.

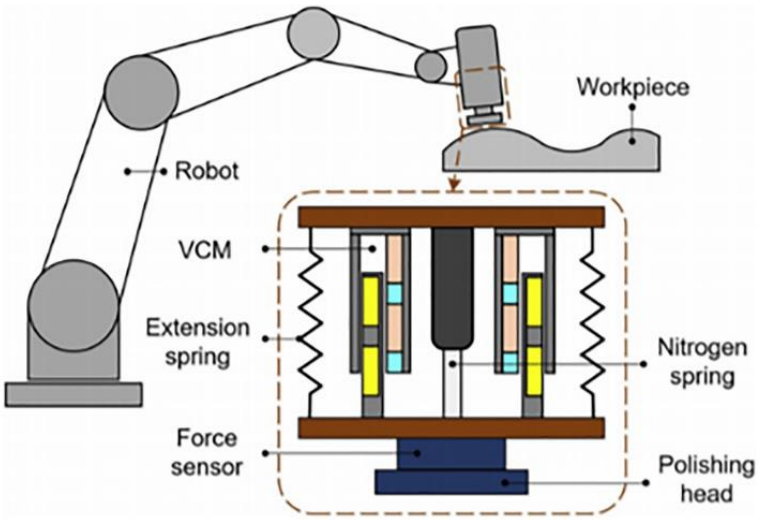

Figure 1: Structure diagram of gas-electric hybrid linear end effector [12]

2. Materials and Methods

This section will present an analysis of the characteristics of a non-Newtonian viscous damper element and the definition of the desired impedance model for the robot's end effector. Subsequently, the formulation will be integrated into the conventional

https://doi.org/10.56038/oprd.v5i1.507

methodology of robotic impedance control. Consequently, a state-space representation will be provided that models the contact dynamics of the end effector of the robot. A qualitative analysis based on the phase portraits for different nonlinear parameters will be presented and discussed to facilitate a more comprehensive understanding of the potential applications of this approach.

2.1. Nonlinear Damping Formulation

In the field of energy dissipation systems, fluid viscous dampers have an important place. These tools are equipped with a chamber, together with a piston and a viscous fluid. When the damper is subjected to motion, fluids viscosity while passing through orifices crate friction which dissipates kinetic energy into heat. The damping force is typically proportional to the velocity of the moving element with higher speeds resulting in greater resistance. Figure 2 shows a standard viscous fluid damper diagram.

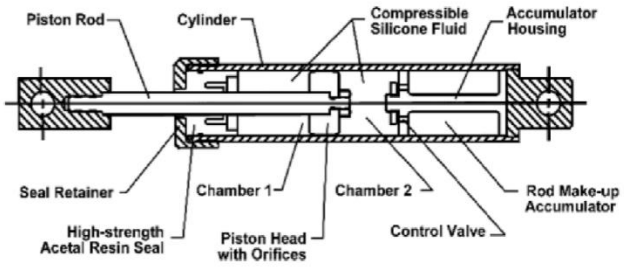

Figure 2: Viscous Fluid Damper [4]

The viscosity of this fluid is often assumed to be in linear and proportional to the sheer strain, which in turn gives the following well-known damping force equation [7]:

$$F = C\dot{x} \tag{1}$$

Where F is the damping force, C is the damping coefficient and $\dot{x}$ is the velocity. This equation assumes that the viscous fluid inside the chamber has a fixed viscosity and thus provides a linear relationship between velocity and damping force. If the fluid in the chamber presents nonlinear viscosity, equation (1) takes the form [8]:

$$F = C\dot{x}^{\alpha} \tag{2}$$

or equivalently;

$$F = Csign(\dot{x})|\dot{x}|^{\alpha} \tag{3}$$

https://doi.org/10.56038/oprd.v5i1.507

Where signum function is defined as,

$$sign(x) = \begin{cases} 1 \; x > 0 \\ 0 \; x = 0 \\ -1x < 0 \end{cases} \tag{4}$$

and the parameter α is an exponential parameter that characterises the non-linear nature of damping. For values bigger than 1, the damping is increased exponentially with velocity, while for values smaller than 1 the damping becomes almost constant with increased velocity. The effects of this parameter can be seen in Figure 3

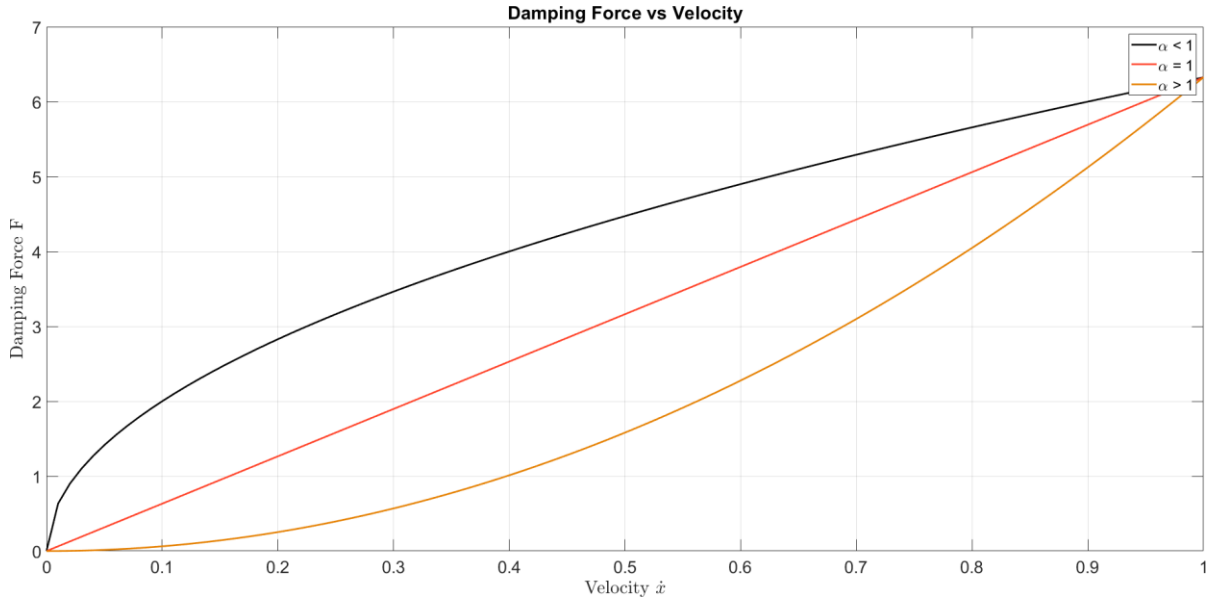

Figure 3: Damping Force and Velocity for Different α Values

2.2. Impedance Control Formulation

The general dynamic equation for a robotic manipulator with n degrees of freedom in joint-space can be written as [9]:

$$B(q)\ddot{q} + C(q,\dot{q})\dot{q} + \tau_f(\dot{q}) + G(q) = \tau - J^T(q)F_{\text{ext}} \tag{5}$$

Where $B(q)$, $C(q,\dot{q})$, τ_f, $G(q)$, τ , F_{ext} corresponds to robot inertia matrix, Coriolis and centrifugal effects matrix, friction torques, gravity torques, torque commands to the robot joints and external forces acting on the end effector respectively. $J(q)$ is the geometric

https://doi.org/10.56038/oprd.v5i1.507

jacobian of the robot while q is the 6x1 vector of generalized joint coordinates in radians. To compensate for the nonlinear terms related to robot dynamics, one can define the control torque τ as;

$$\tau = \hat{B}(q)\alpha + \hat{C}(q,\dot{q})\dot{q} + \hat{\tau_f}(\dot{q}) + \hat{G}(q) + J^T(q)F_{\text{ext}} \tag{6}$$

Where elements with $\hat{*}$ correspond to the identified or estimated counterparts of the real elements. The identification of the robot dynamics is a field of research on its own and parameters can be found using up to date identification techniques such as [11] and [12]. Assuming that there is a perfect compensation, substituting equation (6) into equation (5) yields;

$$\ddot{q} = a \tag{7}$$

Where a is called resolved acceleration in joint-space terms and it will be our control parameter.

The desired end effector contact dynamics can be represented by an impedance model with a standard formulation as

$$K_M\Delta\ddot{X} + K_D\Delta\dot{X} + K_P\Delta X = F_{\text{ext}} \tag{8}$$

Where K_M , K_D and K_P represent nxn diagonal matrices for mass, damping and spring coefficients respectively while $\Delta X = X_d - X$ represents the position error of the robot end effector in cartesian space. Substituting the nonlinear damping in equation (3) to equation (8) we have:

$$K_M\Delta\ddot{X} + K_D sign\left(\dot{X}_d - \dot{X}\right)\left|\dot{X}_d - \dot{X}\right|^{\alpha} + K_P\Delta X = F_{\text{ext}} \tag{9}$$

As can be seen, equation (9) defines the impedance in the cartesian space for the end effector of the robot. This approach makes sense since we are usually dealing with the work being done by the end effector of the robot. Nevertheless, the torque commands are usually being sent to the motors in the joints. Referring back to the equation (7), a transformation should be done to transform this control law into joint space. By using robot kinematics, a in equation (7) can be shown to be equal to

$$\ddot{q} = \text{a} = J^{-1}(q)\left(\ddot{X} - \dot{J}(q,\dot{q})\dot{q}\right) \tag{10}$$

https://doi.org/10.56038/oprd.v5i1.507

Isolating $\ddot{X}$ from equation (9) and substituting into equation (10) gives the control law

$$\tau = \hat{B}(q)\left[J^{-1}(q)\left(\left(\ddot{X}_d + K_M^{-1}\left(K_D sign\left(\dot{X}_d - \dot{X}\right)\left|\dot{X}_d - \dot{X}\right|^{\alpha} + K_P \Delta X - F_{\text{ext}}\right)\right) - \dot{J}(q,\dot{q})\dot{q}\right)\right] + \hat{C}(q,\dot{q})\dot{q} + \hat{\tau_f}(\dot{q}) + \hat{G}(q) + J^T(q)F_{\text{ext}} \quad (11)$$

Equation (11) gives the control torques necessary for the end effector of the robot to have contact characteristics defined in equation (9). One can easily validate this by substituting equation (11) into equation (5). Now focusing on equation (8) and defining state variables as $\mathrm{X} = [\mathrm{X}_1, \mathrm{X}_2]$ where,

$$\mathrm{X}_1 = X^T, \quad X \in R^{1x6}$$
$$\mathrm{X}_2 = \dot{X}^T, \quad X \in R^{1x6}$$

The state space form of the system can be expressed as follows,

$$\dot{X} = \begin{bmatrix} \dot{\mathrm{X}}_1 \\ \dot{\mathrm{X}}_2 \end{bmatrix} = \begin{bmatrix} \mathrm{X}_2 \\ \ddot{X}_d + K_M^{-1}\left(K_D\left(\dot{X}_d - \mathrm{X}_2\right)^{\alpha} + K_P(X_d - \mathrm{X}_1) - F_{\text{ext}}\right) \end{bmatrix} \quad (12)$$

The system represented by equation (12) is that of a non-autonomous, nonlinear mass-spring damper system. It can be seen that the aforementioned formulation negates the terms associated with the nonlinear effects of robot dynamics, leaving us with the system presented with a state space representation. Moreover, the selection of impedance matrices as diagonal matrices facilitates decoupling of the system, thereby enabling independent control of each degree of freedom. This indicates that the vector representations in equation (12) can be omitted, allowing for the analysis of a single degree of freedom system.

As the system represented by equation (12) is non-linear, it is possible to utilize phase portraits [12] in order to gain insight into the behavior of system trajectories for different values of α. By defining $K_M = 1$, $K_P = 10$ and $K_D = 2\sqrt{K_M K_P}$ for critical damping, it is possible to investigate the autonomous behavior of the system with $F_{ext} = 0$ and a constant desired trajectory $x_d = 0$. The phase portraits of the system defined in equation (12) for three different α values 1, 0.5, 2 are presented in Figures 4 to 6.

https://doi.org/10.56038/oprd.v5i1.507

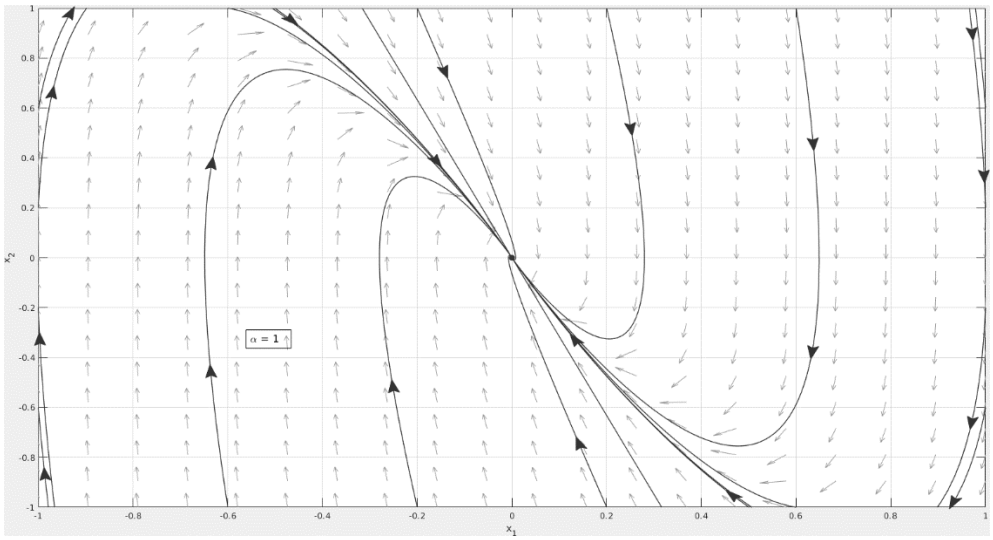

Figure 4: Phase Portraits of the System ($\alpha = 1$)

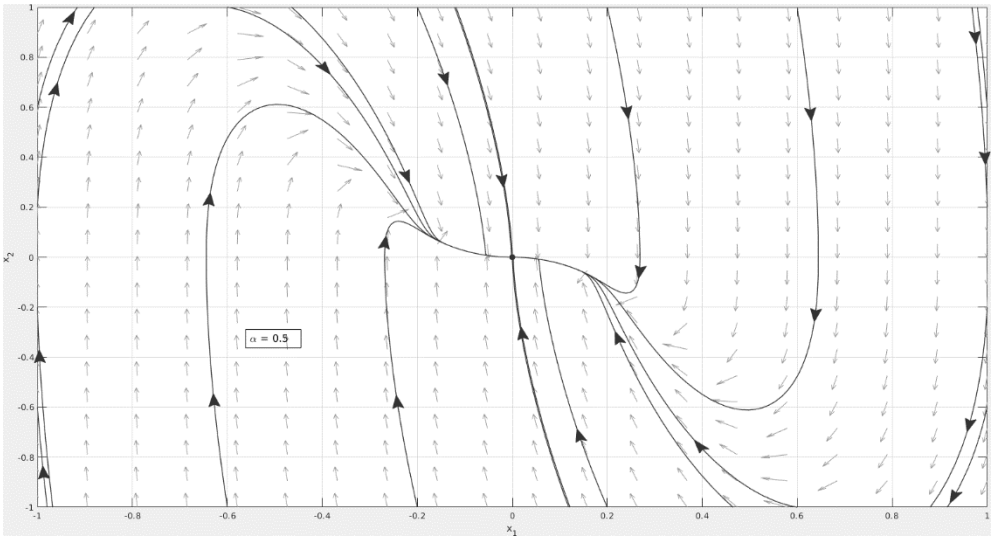

Figure 5: Phase Portraits of the System ($\alpha = 0.5$)

https://doi.org/10.56038/oprd.v5i1.507

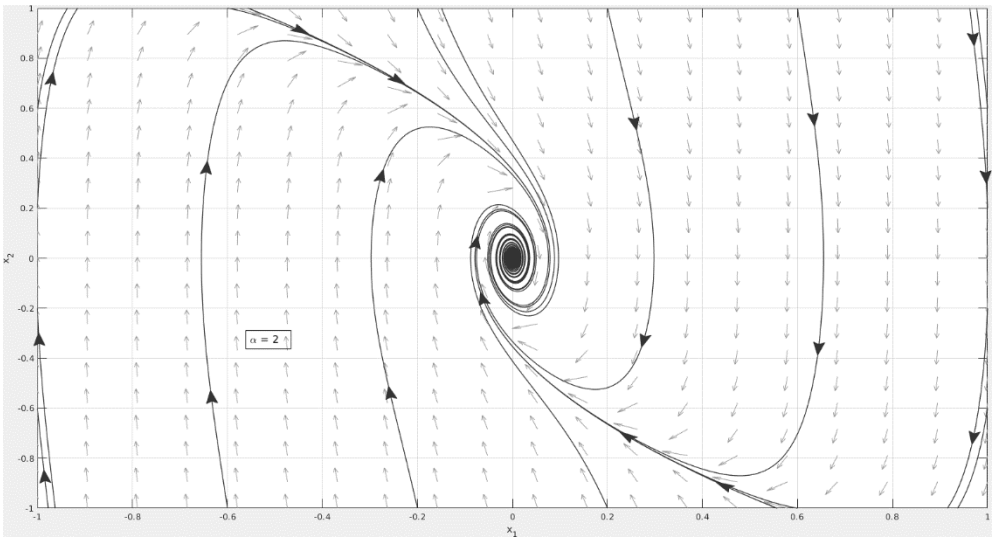

Figure 6: Phase Portraits of the System ($\alpha = 2$)

When the phase portraits presented in Figure 4-6 are carefully examined, we can qualitatively analyze the behavior of the system depending on the variation of the α parameter. First, it can be observed that the system has a single equilibrium point near[1] $x_1 = 0$ and $x_2 = 0$.
Additionally, the nature of the system's oscillations and the characteristics of its approach to the equilibrium point change with variations in the α parameter.

For $\alpha = 0.5$, the phase portrait behaves like a weakly damped system at high speeds. However, as the state trajectories approach the equilibrium point, they exhibit low oscillatory behavior. As the system's speed decreases, the damping force decreases more rapidly than the speed, causing the system to take much longer to reach the equilibrium point. This situation may lead to the formation of a steady-state error in the system.
For $\alpha = 1$, the system exhibits classic critically damped behavior. It demonstrates more stable behavior both at high speeds and near the equilibrium point, leaving no steady-state error.
For $\alpha = 2$, the damping in the system increases exponentially with speed. As a result, high speeds are damped much more quickly. However, near the equilibrium point, the

[1] The precise equilibrium points can be quantatively calculated by setting $\begin{bmatrix} \dot{X}_1 \\ \dot{X}_2 \end{bmatrix} = \begin{bmatrix} 0 \\ 0 \end{bmatrix}$ and solving the nonlinear differential equation in equation (12)

https://doi.org/10.56038/oprd.v5i1.507

system's trajectories tend to exhibit spiral behavior. This condition may shift the equilibrium point from a stable node to a stable focus.

3. Result

The method presented above can be applied to a variety of scenarios. This study focuses on two specific cases. The first case concerns a collaborative robotic polishing application, where the vibrations generated by the polishing tool must be compensated for while maintaining the robot's flexibility to handle large, unexpected collisions or human contact. The second case examines a free-drive application, where the robot is required to achieve precise positioning while resisting velocity exponentially to ensure safety. The simulations are conducted using equation (12) and MATLAB numerical ode solvers.

3.1. Case 1

For this application, we can think of a polishing tool attached to the end effector of the robot. The external forces that this tool applies to the robot can be modelled as a periodic function, such as,

$$F_{tool} = A_{Vibration}\, cos(2\pi\omega t) \tag{13}$$

Where $A_{Vibration}$ represents the amplitude of the applied force in newtons (N), and ω denotes the vibration frequency in hertz (Hz). Assuming the polishing tool operates at a rotational speed of 3000 revolutions per minute (rpm), corresponding to a frequency of 50 Hz, and the amplitude of the applied force is 1 N, the resulting position response at the end-effector is depicted in Figure 7.

https://doi.org/10.56038/oprd.v5i1.507

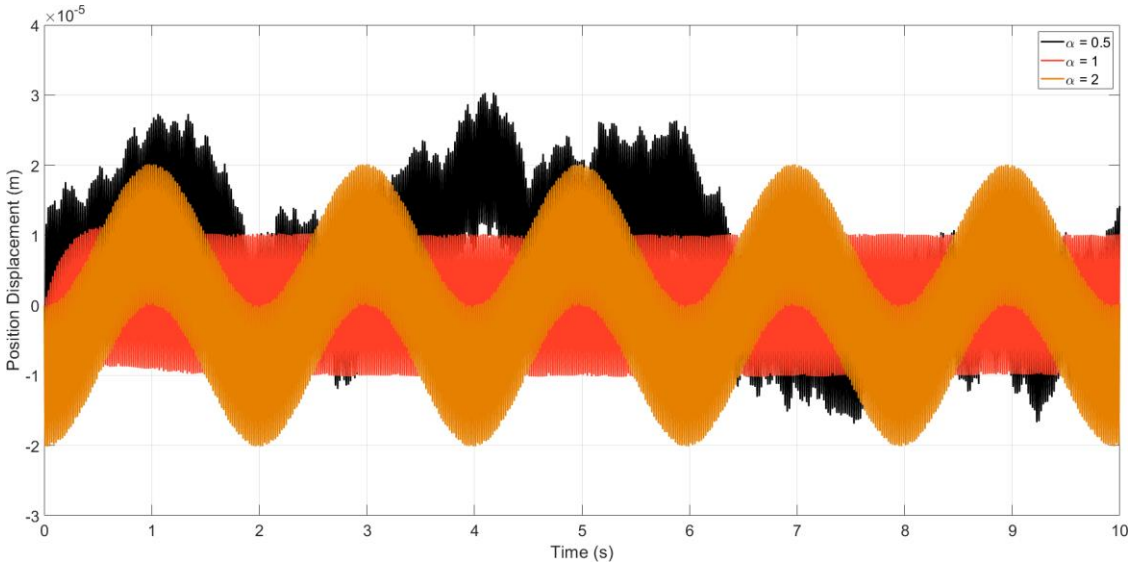

Figure 7: Positional Displacement of the System Under Vibration for Different Values of α

Figure 7 illustrates that the response and deviation from the equilibrium position remain relatively consistent across different values of α. This indicates that the system effectively dampens high-frequency, low-amplitude vibrations to a similar degree, regardless of the variation in the exponential parameter.

Consider now a scenario where an unexpected collision occurs between a human and the robot at the 2-second mark with a magnitude of 50 N. This can be modelled as an impact input to the system, designated as,

$$F_{impact} = A_{impact}\delta(\mathrm{t} - \mathrm{t_{impact}}) \tag{14}$$

Where A_{impact} = 50N and t_{impact} is 2 s. By superposing equations (13) and (14), it is possible to create a model of the collision while the tool is subjected to vibration.

$$F_{ext} = F_{tool} + F_{impact} \tag{15}$$

Subsequent to this impact, the positional displacement of the system is modified and is expressed as follows:

https://doi.org/10.56038/oprd.v5i1.507

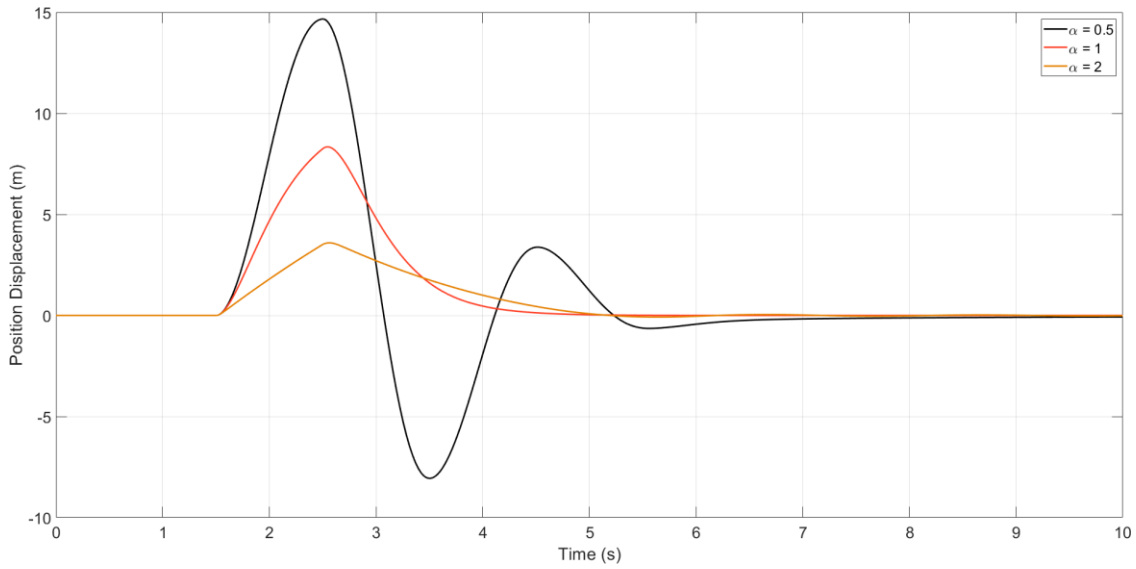

Figure 8: Positional Displacement of the System in Impact for Different Values of α

As shown in Figure 8, the system's impact characteristics exhibit increased flexibility when $\alpha < 1$, whereas values of $\alpha > 2$ result in a stiffer response. In a scenario where the robot collides with a human, it is desirable for the robot to be as flexible and adaptive as possible. In such cases, selecting a value $\alpha < 1$would enable the desired flexibility, while maintaining the same vibration damping capabilities as demonstrated in Figure 7.

3.2. Case 2

In this case, we will assume that a human operator is recording some points using the free drive function of the robot. In this scenario, the human operator may apply a constant force of 10N to the end effector, beginning at the two-second mark. At the six-second mark, the human operator may apply an excessive and exponential force to the robot. The constant force can be modelled as follows:

$$F_{cnst} = A_{const} \tag{16}$$

Where $A_{cnst} = 10$. At the two-second mark, the excessive human force can be modelled as an exponential input as,

$$F_{exp} = A_{exp} e^{\lambda(t - t_{exp})} \tag{17}$$

https://doi.org/10.56038/oprd.v5i1.507

Where $A_{exp} = 10$ and $\lambda = 2$. Super positioning equation (16) and (17), the response of the end effector velocities can be seen in Figure 9 below.

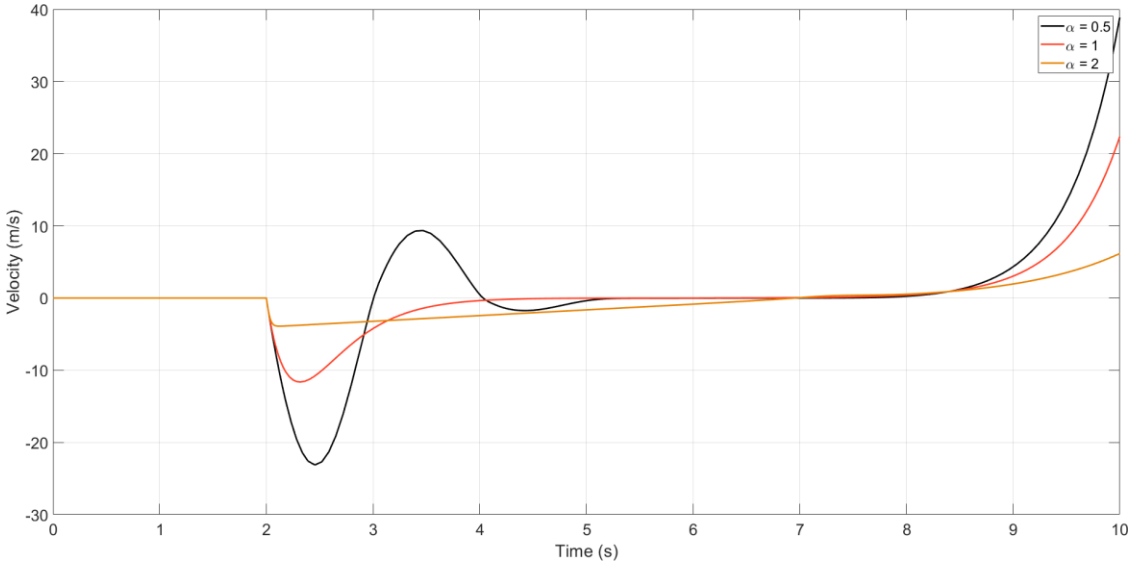

Figure 9: Velocity of the End Effector for Different Values of α

The velocity response of the system reveals that for values of $\alpha < 1$ or $\alpha = 1$, the velocity of the end effector increases exponentially in response to an exponential input. However, for values of $\alpha > 1$, the system's response is significantly more stable, providing a safer condition even when the force input is exponential. This indicates that, even with values greater than 1, the operator can still easily manipulate the end effector to the desired position by applying small amounts of force, while the system autonomously stabilizes in the event of excessive force. This behavior aligns with the desired functionality of a robot in free drive.

4. Discussion and Conclusion

The findings of this study indicate that there are encouraging enhancements in the functionality of robotic systems when they are subjected to environments with varying levels of force and interaction. The incorporation of a non-Newtonian fluid-based damping element into the conventional robotic impedance control framework confers a distinctive advantage over conventional damping methodologies. By arranging the exponential parameter, the robot is able to adaptively select between exponential and

logarithmic damping, thereby enabling it to achieve the specific stability and safety requirements of a given task.

Nevertheless, a number of challenges remain. A significant challenge arises from the incorporation of a non-linear term into the impedance equation, which introduces additional complexity. A stability analysis and proof for such a system would represent a significant avenue for future research, with the aim of aligning with the established frameworks set out in works such as [14]. Furthermore, the selection of the most appropriate exponential parameter, in conjunction with the impedance coefficients for specific tasks, requires further investigation. The learning of variable impedance parameters for different tasks has been extensively studied, with examples in [15] and [16]. These studies could be expanded to include the non-linear term in the equation. Moreover, while the proposed solution offers enhancements in vibration damping, further investigation is required to ascertain the scalability of these effects in more intricate and dynamic real-world scenarios, particularly in applications where known vibrations must be mitigated while maintaining the robot's flexibility.

5. Acknowledge

This work was supported by the private organization MCFLY Robot Technologies. I would like to express my sincere gratitude to all the team members for their invaluable contributions and support throughout the project. I also extend my thanks to my master's advisor Semih SEZER for their insightful guidance and constructive feedback.

References

[1] Hogan, Neville. "Impedance control: An approach to manipulation." 1984 American control conference. IEEE, 1984.

[2] Chang, Pyung Hun, and Maolin Jin. "Nonlinear target impedance design and its use in robot compliant motion control with time delay estimation." IECON 2006-32nd Annual Conference on IEEE Industrial Electronics. IEEE, 2006.

[3] Lai, Chow Yin, et al. "Nonlinear damping for improved transient performance in robotics force control." 2012 IEEE/ASME International Conference on Advanced Intelligent Mechatronics (AIM). IEEE, 2012.

[4] Gherbi, A., and M. Belgasmia. "Use of fluid viscous dampers in structural control: a case study." International Journal of Forensic Engineering 4.2 (2018): 119-132.

[5] Kim, Dae Wook, and James H. Burge. "Rigid conformal polishing tool using non-linear visco-elastic effect." Optics express 18.3 (2010): 2242-2257.

[6] Golzar, F., Geoff Chase, and G. Rodgers. "Experimental testing of a re-centring viscous damper with non-Newtonian damping fluid." (2019).

https://doi.org/10.56038/oprd.v5i1.507

[7] Makris N, Constantinou MC, Dargush GF. Analytical model of viscoelastic fluid dampers. Journal of Structural Engineering. 1993 Nov;119(11):3310-25.

[8] Paola, M. Di, L. La Mendola, and G. Navarra. "Stochastic seismic analysis of structures with nonlinear viscous dampers." Journal of Structural Engineering 133.10 (2007): 1475-1478.

[9] B. Siliciano, L. Sciavicco, L. Villani, G. Oriolo, "Robotics: Modelling, planning and control," New YorN, NY, USA: Springer, 2010.

[10] M. Gautier, S. Briot, "Global identification of joint drive gains and dynamic parameters of robots," Journal of Dynamic Systems, Measurement, and Control, vol. 136, no. 5, p. 051 025, 2014

[11] M. Tang, Y. Yan, B. An, W. Wang, Y. Zhang, "Dynamic parameter identification of collaborative robot based on wls-rwpso algorithm," Machines, vol. 11, no. 2, p. 316, 2023.

[12] H. K. Khalil, Nonlinear systems; 3rd ed. Upper Saddle River, NJ: Prentice-Hall, 2002

[13] Liangjian O, Miao Y, Xiaolu H, Shuheng Q, Chi Z, & Kai F (2021) Design of a Pneumatic-Electric Hybrid Linear End-efector for Robot Polishing. 2021 13th International Symposium on Linear Drives for Industry Applications, 6 https://doi.org/10. 1109/ldia49489.2021.9505754

[14] Kronander, Klas, and Aude Billard. "Stability considerations for variable impedance control." IEEE Transactions on Robotics 32.5 (2016): 1298-1305.

[15] Alhousani, Naseem, et al. "Geometric reinforcement learning for robotic manipulation." IEEE Access (2023).

[16] Abu-Dakka, Fares J., and Matteo Saveriano. "Variable impedance control and learning—a review." Frontiers in Robotics and AI 7 (2020): 590681.